ARTICLE

A Way To Control the Gold Nanocrystals Size: Using Seeds with Different Sizes and Subjecting Them to Mild Annealing

Nicolas Goubet,[†] Yong Ding,[‡] Mathias Brust,[§] Zhong Lin Wang,[‡] and Marie-Paule. Pileni[†,*]

[†]Université Pierre et Marie CURIE, UMR 7070, LM2N, 4 Place Jussieu, 75005 Paris, France, [‡]School of Materials Science and Engineering, Georgia Institute of Technology, Atlanta, Georgia 30332-0245, and [§]Department of Chemistry, The University of Liverpool, Crown Street, Liverpool, U.K. L69 7ZD

ABSTRACT We demonstrate that the sequence of reactants plays a key factor in the final size of Au nanocrystals. The growth mechanism markedly differs with seed size and/or internal crystallinity. Conversely to what could be expected when the multiple-twinned particle (MTP) seeds are rather large (3.5 nm) they control the nanocrystal growth. When the single domain seeds are very small (1.5 nm) the majority of nanocrystals produced are large icosahedral (85%) nanoparticles as predicted from a theoretical model.

KEYWORDS: gold · nanocrystals · annealing · icosahedron · melting

Much attention has been paid over the past decade to noble metal nanocrystals because of their potential use as advanced materials in new electronic and optical devices. Reduction of the size of noble metals down to a nanometric scale is accompanied by large modifications in their optical properties, including the appearance of new resonances. The possibility of adjusting the surface plasmon resonances by modifying the size, shape, structure, and the environment of these nanocrystals has been the focus of this research for much of 10 years.[1,2]

Various chemical methods have been developed to control the size and shape of these nanocrystals by changing the preparative conditions such as the kind and/or the amount of protecting agent.[3,4] In many cases the same synthesis does not produce the same final size and shape. This phenomenon may be attributed to either the presence of some impurities, and/or additives, present in a very low concentration in the reactants.[5] Most of the syntheses reported in the literature give very few details of the various steps of the chemical reaction.[3]

Gold nanocrystal syntheses have been extensively studied during the past decade.[6] A rather large number of groups have carried out thermal treatments of Au nanocrystals with the view of controlling the size, shape, and size distribution:[7−13] The control of nanocrystal size in the nanometer range, with a rather large size distribution, is obtained either by changing the molar ratio of gold to alkanethiol,[8] by annealing from 150 to 250 °C in air,[9] or *via* a thermal process in which the chain length and the concentration of the alkylthiols is manipulated.[10] In the last case, a quantitative correlation between size selectivity and these two parameters is established. Control of size and shape can also be accomplished by thermal treatment in solution.[11] The size distribution is controlled by a process called digestive ripening, which consists in heating a colloidal suspension at or near the solvent boiling point in the presence of a surface active ligand.[12] Rather large (220 nm) icosahedral nanocrystals are obtained by thermal processing in the aqueous phase.[13]

In this paper, we demonstrate that the crystal growth mechanism of gold nanocrystals markedly changes with the sequence of reactants added during the synthesis. We have also proposed growth mechanisms to explain the observed phenomenon.

RESULTS AND DISCUSSION

Let us first recall that many symmetric clusters can be constructed from the close packing of hard spheres. With fcc gold crystals, the clusters, considered as compact packing of spheres, are cubooctahedra, decahedra, and icosahedra. The surface of a cubooctahedral cluster consists of eight (111) planes and six (100) planes with closed atomic shells. The cuboctahedron represents the most stable form. The decahedra and icosahedra are structures with 5-fold symmetry and are called multiple-twinned particles (MTP). In fact, decahedral clusters consist of five deformed tetrahedral sub-

*Address correspondence to pileni@sri.jussieu.fr.

Received for review July 2, 2009 and accepted October 8, 2009.

Published online October 15, 2009.
10.1021/nn9007274 CCC: $40.75

units twinned by their {111} planes, whereas icosahedral clusters originate from the twinning of 20, (111) faces, deformed
tetrahedral subunits.

Syntheses of Au seeds with different sizes are described: The main difference between them is related to the sequence of reactant addition during the chemical process. The reactants remain unchanged as do their concentrations and the volume of the vessel used to produce the nanocrystals. To prevent coalescence, nanocrystals need to be coated by a surfactant (or polymer). Here dodecanethiol molecules are used as the coating agent and are bound to the Au surface *via* a quasi-covalent bridge. The syntheses described below are highly reproducible and based on the revisited Brust−Schiffrin method that is known for its ability to produce a large amount of nanocrystals.[7] Briefly, an aqueous solution (30 mL) containing 3 mM $HAuCl_4 \cdot 3H_2O$ is added to 50 mM of tetradecylammonium bromide (TDAB) in 80 mL of toluene. After 10 min stirring, the organic phase turns orange, the colorless aqueous phase is then removed. It is after this step that the synthesis varies:

(i) Procedure I: 1 mL of 1-dodecanethiol ($[C_{12}SH] = 4.2.10^{-3}$ mol/L) is added to the organic phase. The orange organic phase turns colorless, as has been observed.[14] This color change is attributed to formation of a polymeric Au(I) thiolate species. Sodium borohydride ($[NaBH_4] = 0.4$ mol/L) in aqueous solution (25 mL) is then added and the biphasic phase is stirred for 3 h after which the aqueous phase is removed.

(ii) Procedure II: Instead of adding dodecanethiol before the chemical reduction, as in procedure I, 25 mL of 0.4 M sodium borohydride ($NaBH_4$) solution is added first, and the solution is then stirred for 3 h. The aqueous phase is removed, and 1 mL of 1-dodecanethiol is added to the organic phase.

In both cases the solvent is removed and the crude solid is dried under vacuum overnight and then dissolved again in 5 mL of toluene. At the end of the synthesis a drop of solution is deposited on a TEM grid covered by amorphous carbon. From procedure I, as shown by the Figure 1 inset, there is formation of rather small nanocrystals with an average diameter of 1.5 nm and a 25% size distribution. This is in good agreement with published data.[9] The high resolution transmission electron microscopy (HRTEM) image shows that most of the nanocrystals are characterized by a single crystalline phase corresponding to cubooctahedra (Figure 1).

From procedure II, as shown in Figure 2A, there are rather large and highly crystalline nanoparticles (3.5 nm) with a 20% variation in the size distribution. The dark-field image (Figure 2B) shows that only parts of the nanocrystals are diffracting, indicating multiply twinned (MTP) particles formation. The bright butterfly-like patterns correspond to the presence of well-oriented icosahedral nanoparticles (see later).

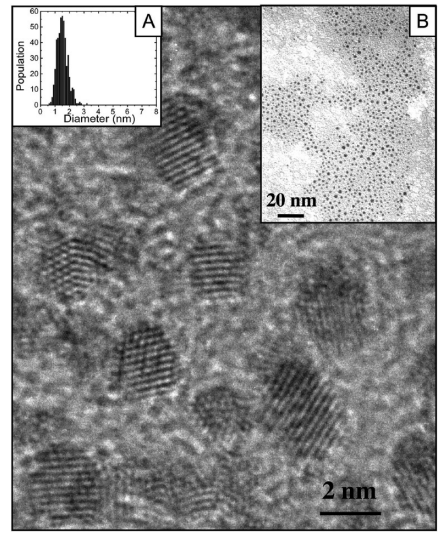

Figure 1. High resolution TEM image of seeds I. The insets display the TEM image over a long distance and the nanocrystal size distribution.

Hence, by changing the period at which dodecanethiol is added, the final size and crystallinity of Au seeds change. As described above, at the end of each synthesis, seeds having different average sizes (1.5 and 3.5 nm) and crystallinities (cubooctahedral and icosahedral), called seeds I and II for simplicity, respectively, are produced. In the following, the two different seeds dispersed in toluene are subjected to the same annealing treatment. The solution is annealed progressively in air with a heating rate of $10\ K \cdot min^{-1}$. After 16 min the solution temperature reaches 463 K and it is kept at this temperature for 30 min. At 463 K, toluene is evaporated ($T_{boilling} = 383$ K), the surfactant (TDAB) is now in the liquid state ($T_{melting} = 353$ K), and the solution turns orange with the appearance of a black precipitate. The colloidal solution is left in the laboratory and returns slowly to room temperature. At the end of the process the dark precipitate is trapped in a viscous orange solution. Note, by following the same procedure as described above in the absence of $HAuCl_4 \cdot 3H_2O$, the viscous orange liquid is still formed indicating that a complex chemical reaction between the two surfactants (TDAB and $C_{12}SH$) and the $NaBH_4$ takes place to form this colored byproduct. Toluene (10 mL) is then

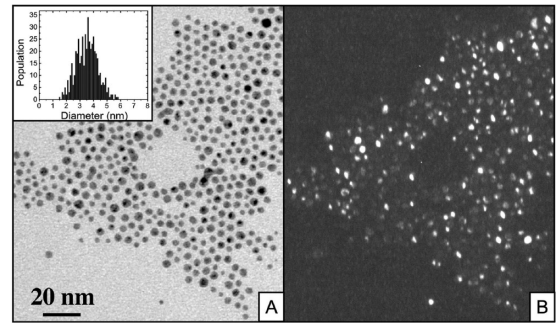

Figure 2. (A) Bright-field and (B) dark-field image of seeds II. The inset displays the nanocrystals size distribution.

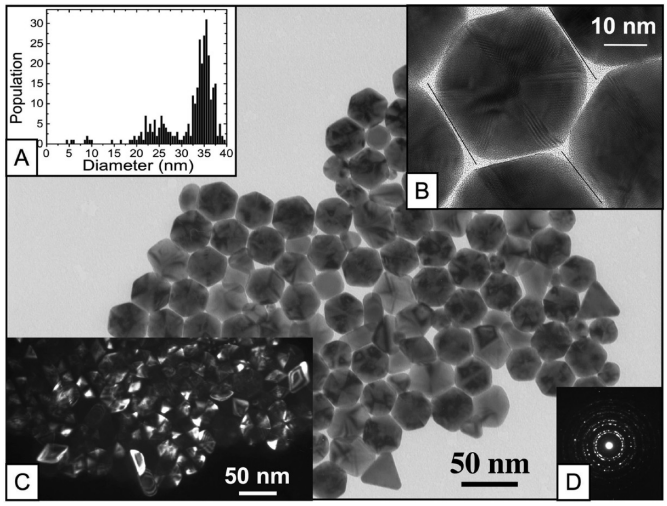

Figure 3. TEM images of the annealed seeds I. Size distribution (A), high resolution (B), dark-field (C) and electron diffraction (D) of the resulting nanocrystals.

added to the solution, and the nanocrystals are progressively precipitated with the addition of ethanol. After removing the supernatant solution, the precipitate is dispersed in hexane (6 mL) and a drop of solution is deposited on a TEM grid. Figure 3 shows that seeds I, subjected to the annealing process as described above, produce 85% very well faceted hexagonal particles, 9% triangular, and 6% pentagonal nanoparticles. The size distribution (Figure 3 insert), assuming a diameter of the circle surrounding each particle, is bimodal with average diameters of 25 and 35 nm, respectively. Note that small nanocrystals with a diameter in the range of a few nanometers (from 4 to 10 nm) are still present.

To characterize the structures of these nanoparticles with different shapes, bright- and dark-field images are obtained of isolated nanoparticles (Figure 4). The hexagonal shaped nanoparticles are characterized by six diffraction spots of corresponding {111} planes, forming an angle of 60° between them (Figure 4A). The dark-field image of one spot shows bright butterfly-like patterns (Figure 4B). Similarly, the dark-field images of the other two spots also show illumination of the two other series of [111] orientations (Figure 4C,D). This is consistent with an icosahedral crystal on the 3-fold axis.[15] The HRTEM image shows that the {111} planes of icosahedral particles are in front of their neighbors (Figure 3B). Formation of single crystal octahedrons oriented in the [111] axis can be eliminated because the overall particle is not equally imaged owing to the change in the diffracting condition and particle orientation. Pentagonal nanoparticles (Figure 4E) are characterized by two diffractions corresponding to the {111} and {220} reflections in the same direction (Figure 4F). The corresponding dark-field image of {111} reflections shows nonuniform brightness due to the variation in the projected thickness of the segment of the particle that is being imaged (Figure 4G). This is confirmed by the dark-field image of the {220} reflection where the illuminated part (Figure 4H), shows some equal thickness fringes that reveal a 3D shape like a tetrahedron oriented along [111]. From this it is concluded that pentagonal particles are in fact decahedra seat on one of these {111} faces. The triangular shape (Figure 4I) shows two pairs of {111} and one of {200} reflections (Figure 4J) with a bright dark-field image (Figure 4K), indicating formation of a single crystal as already observed.[16,17] Some elongated particles in the monolayer (Figure 4L) are also seen. By tilting the sample by 32° (Figure 4M), the elongated crystals show a tilted triangle indicating that they are, in fact, triangular single crystals sitting on their edges. From this structural study we concluded that 85% icosahedral, 9% triangular, and 6% decahedral crystals were produced. Thus, thermal treatment of 1.5-nm cuboctahedral Au nanocrystals induces formation of large icosahedral particles.

By replacing seeds I (1.5 nm) by II (3.5 nm) dispersed in toluene and subjecting them to the same thermal treatment as described above, Au nanocrystals with local and long-range ordering are observed (Figure 5A and insert). The average diameter and variation in size distribution are 5.8 nm and 9%, respectively (Figure 5A insert). The dark-field image (Figure 5B) corresponding to Figure 5A shows well-defined nanocrystals with various contrasts, indicating the formation of MTP. Figure 5 panels C and D show the same image at a larger magnification with the appearance of a very large number of butterfly-like patterns, corresponding to 111 diffraction spots of hexagonal particles[15] and indicating formation of icosahedral nanoparticles. This is confirmed by HRTEM with the appearance of well-defined icosahedral particles (Figure 5E,F). Hence, the

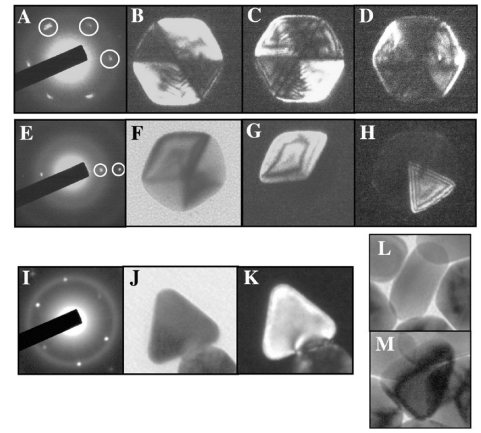

Figure 4. Diffraction pattern (A), dark-field images (B, C, and D) formed by using 111 reflections of hexagonal particles. Diffraction pattern (F), bright- (E) and dark-field images (G and H) formed by using 111 and 220 reflections of pentagonal particles, respectively. Diffraction pattern (J), bright- (I) and dark-field (K) image formed by using 111 reflections of triangular particles. Elongated nanocrystals at tilt 0° (L) and tilt 32° (M).

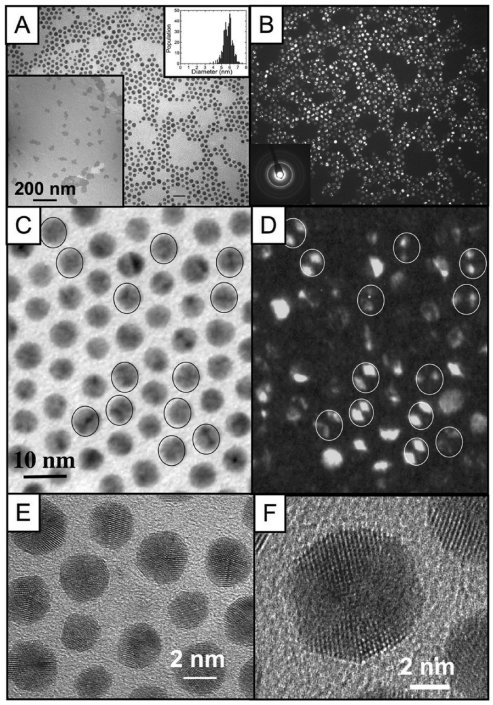

Figure 5. TEM images of the annealed seeds II. Bright-field (A) (size distribution inset) and dark-field image (B), local bright-field (C) and dark-field (D) and high resolution (E,F) of the resulting nanocrystals.

size of the seeds for thermal treatment induces formation of mainly icosahedral nanocrystals differing markedly by their sizes. These alterations in the final Au nanocrystal size raise an interesting question. Is it possible to control the nanocrystal size by mixing the seeds of different sizes? To answer this question, the 1.5-nm and 3.5-nm nanocrystals produced as described above are mixed in various proportions. The thermal treatment is performed as above. At the end of the synthesis a drop of solution is deposited on a TEM grid. In going from Figure 6A to Figure 6D, the TEM images correspond to syntheses carried out on increasing the relative amount of 1.5 nm cubooctahedral seeds. Because the size distribution is very low (6%−8%) large monolayers are observed. Conversely to what was expected, the increase in the nanocrystals size with an increase in the percentage of 1.5-nm seeds is very slight (Figure 6E) with a very low size distribution. From the data given above it can be concluded that the presence of even a very low amount (5%) of the large seed size (3.5 nm) favors the formation of relatively small nanocrystals (5.3−8 nm), with a very low size distribution favoring the Au nanocrystals long-range ordering.

As the seeds are dispersed in toluene it is rather difficult to give direct proof of the growth mechanism during the annealing process. Nevertheless, a tentative explanation can be given taking into account data obtained with seeds I and II deposited on a TEM grid covered by a rough surface of amorphous carbon and subjected to annealing under the same thermal conditions as described earlier. After maintaining the TEM grid at 463 K for 30 min, the sample is cooled to room temperature. For 1.5-nm cubooctahedral seeds (I), as shown in Figure 7A, the nanocrystals remain isolated on the substrate with an average size slightly larger than that of the seeds before annealing (4.7 ± 0.9 nm). However, very surprisingly, conversely to what is usually observed, with an improvement in the nanocrystallinity by annealing, the internal structure of the seeds evolves from cubooctahedral to a mixture composed of polycrystalline (see arrows in Figure 7A) and cubooctahedral nanoparticles. The calculated melting point of 1.6-nm Au particles, 500 K,[18] is very close to that of the thermal treatment (463 K) imposed on the 1.5-nm Au seeds. Because of the presence of a rather large size distribution (Figure 1 insert) it is reasonable to assume that most of the seeds are completely melted with a rather small proportion being in the premelting process. This change in nanocrystallinities (Figure 7A) with the appearance of a polycrystalline phase in coexistence with the cubooctahedral nanoparticles (see arrow) is a straightforward proof that some of the seeds (I) melt during the thermal treatment and recrystallization takes place during the cooling.

This is consistent with the decrease in the nanoparticle melting temperature, observed

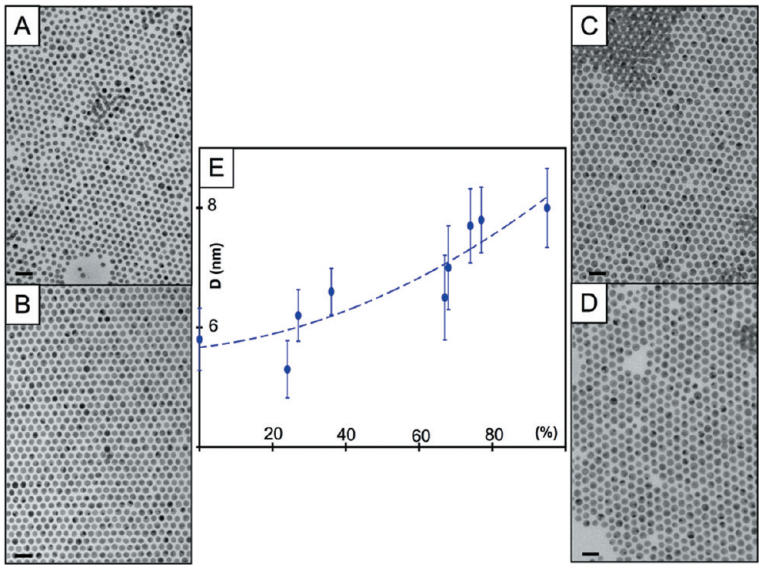

Figure 6. Relationship between the final nanocrystals size and the percentage of 1.5 nm precursors in the mixture before annealing (E), 25% (A), 33% (B), 67% (C), and 75% (D).

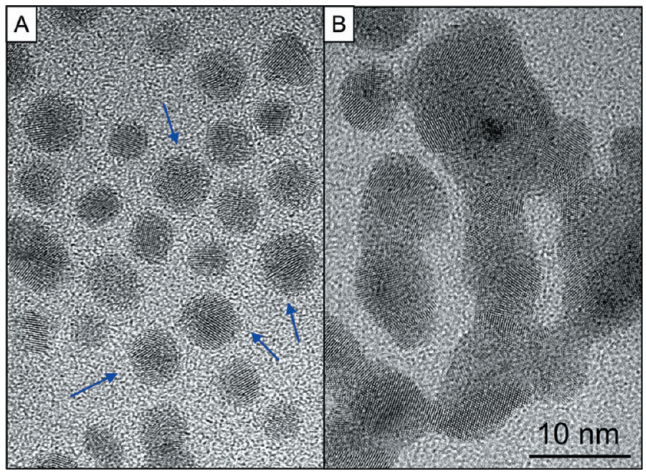

Figure 7. TEM image of seed I (A) and II (B) deposited on amorphous carbon and submitted to the same thermal treatment as those in solution.

experimentally[19,20] and from calculation,[18] with the particle size. Note that it is consistent with the crystallization process in the cooling of 4-nm liquid Au particles, followed by molecular dynamics simulation,[18] from which the polycrystalline fcc structure is considered as the most energetically stable structure of Au particles. The Au nanocrystals sizes remain in the same order of magnitude (4.7 nm) compared to the seeds (1.5 nm) as observed in Figure 7A. This slight increase in the nanoparticle size by thermal treatment can be explained as follows: the smallest nanoparticles melt and the liquidlike clusters tend to diffuse on the substrate. However this diffusion process is reduced by the strong interaction between atoms and small clusters on the substrate.[21] For the larger particles (above to 1.5 nm), the core of the nanocrystals remains solid whereas the adatoms tend to melt and strongly interact with the substrate inducing an increase in the nanoparticle size. On increasing the seed size to 3.5 nm (seeds II), the calculated melting point is estimated to be 950 K.[18] The thermal treatment of seeds II (3.5 nm) deposited on a TEM grid as described above with seeds I shows coalescence of the seeds over a very large area (Figure 7B) with either nanocrystals stuck together or as ramified islands. Such behavior is expected because the diffusion of large Au clusters is rapid on graphite surfaces and the increase in the diffusion with the cluster sizes.[21−24] These data are consistent with the liquid shell model where the freezing of molten particles gives rise to icosahedral nanoparticles considered as the most stable structure.[25] From these results it is concluded that 3.5-nm Au seeds *dispersed in solution* and subjected to mild annealing (463 K) do not melt. As has been demonstrated[25] experimentally and from molecular dynamics, large clusters diffuse rapidly to minimize surface energy. This diffusion is described as a Brownian motion induced by the internal vibrations of the cluster and/or the vibrations of the substrate. This explains the rather large number of Au {111} surfaces as MTPs.

From the data collected above we have concluded that when a thermal treatment is employed, the mechanism of Au nanocrystal growth markedly differs with the seed size. Small seeds subjected to this thermal treatment reach a liquidlike phase, which leads to the formation of mainly large icosahedral particles which are the most stable Au fcc structures. Conversely, when the seed size is larger, they no longer melt, and migration of atoms/adatoms between nanocrystals becomes the predominant growth and shaping mechanism. To a first approximation, it is reasonable to claim that during the annealing process the nanocrystals melt as the surfactant (353 K). As mentioned above, after annealing at 463 K the sample is left in the laboratory without any precautions. This favors a slow cooling rate and consequently formation of ordered nanosurfaces with a 5-fold symmetry. By simulation[25−27] it is found that crystallization of the interior atoms as well as the external ones leads to an icosahedral structure. The finding that, at equilibrium, the Au nanoparticles consist of 85% icosahedral particles is explained by the fact that the Au (111) surface has the lowest surface energy.[25] This confirms that the kinetics of nucleation and growth in clusters play a key role in determining the structure of the nanocrystals and various forms can be produced under identical conditions due to the stochastic nature of nucleation.[18,25] This explains why other shapes are produced as well. From this, it is concluded that small cubooctahedra (1.5 nm) melt during the thermal treatment and a slow cooling rate favors formation of large icosahedral nanocrystals with the presence of small amounts of other structures.
Conversely to what was expected, the increase in the nanocrystals size with increasing the percentage of 1.5-nm seeds is very slight (Figure 6E) with a very low size distribution. Hence, even with a rather large amount of 1.5-nm seeds (95%), large Au nanocrystals are not produced. Thus the annealing mechanism of a mixture of 1.5-nm and 3.5-nm seeds (I and II, respectively) can be explained as follows: During the thermal treatment, seeds (I) melt with formation of liquidlike particles that prefer to adhere to the {111} faces of MTP solidus larger particles (seeds II) with a minimization of energy inducing a slight increase in the nanocrystals sizes with a very low distribution. The drastic change in the final nanocrystals size with small seeds compared to what is obtained with either larger ones or a mixture of the two (I and II) indicates that it is energetically more difficult to produce new solidus nanocrystals from

molten particles than to adhere to existing solidus nanocrystals.

CONCLUSIONS

The seed size is the key parameter in the final structure: 1.5-nm cubooctahedral seeds coalesce to produce large icosahedral nanocrystal nanoparticles, whereas 3.5-nm icosahedral seeds produce 5.8-nm nanocrystal icosahedra. From the two syntheses described above, the precursors having various structures (cuboctahedron and MTP) make it possible to reach the same final shape as MTP particles with various sizes. For example, ~13000 cubooctahedral nanocrystals with 1.5-nm average size coalesce during the heating process to produce large (25−35 nm) icosahedral nanocrystals. By changing the reactant sequence, the 3.5-nm icosahedral nanocrystals become larger nanocrystals (5.8 nm) but with the same structure, indicating a homogeneous growth in the reactive medium. This shows that two different nanocrystal growth mechanisms take place by changing the sequence in the chemical reaction and that this is mainly related to the size of the nanocrystals subjected to a thermal treatment. This finding may be of relevance in the preparation of several types of nanoparticles besides gold, for example, silver, platinum, and palladium.

METHODS SECTION

Materials. All products and solvents were from a variety of sources and used without purification: tetrakis(decyl)ammonium bromide (TDAB) (Aldrich, >99%), hydrogen tetrachloroaurate(III) hydrate (Aldrich, 99.9%), toluene (Riedel-deHaën, >98%), 1-dodecanethiol (Aldrich, >98%) and sodium borohydride (Aldrich, 99%). The water used was purified with a Milipore system (18.2 MΩ).

Characterization. The conventional transmission electron microscopy observations were made using a Jeol 1011 at an accelerating voltage of 100 kV. Electron diffraction, bright- and dark-fields were used to characterize the structure and shape of the Au nanocrystals. The high-resolution transmission electron microscopy study was carried out at 400 kV using a JEM 4000EX.

The Au nanocrystals coated with 1-dodecanethiol and dispersed in toluene were deposited on conventional electron microscopy grids covered by an amorphous carbon film.

Acknowledgment. We thank Dr. I. Lisiecki, Dr. A. Ngo, and Dr. C. Salzemann for fruitful discussions. The research leading to these results has received funding from the European Community's Seventh Framework Programm (FP7/2007-2013) under Grant Agreement No. 213382.

REFERENCES AND NOTES

1. Brioude, A.; Jiang, Y.; Pileni, M. P. Optical Properties of Gold Nanorods: DDA Simulations Supported by Experiments. *J. Phys. Chem. B* **2005**, *109*, 13138–13142.
2. Arbouet, A.; Voisin, C.; Christofilos, D.; Langot, P.; Del Fatti, N.; Vallée, F.; Lerme, J.; Celep, G.; Cottaman, E.; Gaudry, M.; Pellarin, M.; Broyer, M.; Maillard, M.; Pileni, M. P.; Treguer, M. Electron-Phonon Scattering in Metal Clusters. *Phys. Rev. Lett.* **2003**, *90*, 177401-1–177401-4.
3. Pileni, M. P. Control of the Size and Shape of Inorganic Nanocrystals at Various Scales from Nano- to Macrodomains. *J. Phys. Chem. C* **2007**, *111*, 9019–9038.
4. Pileni, M. P. Role of Soft Colloidal Templates in the Control of Size and Shape of Inorganic Nanocrystals. *Nat. Mater.* **2003**, *2*, 145–150.
5. Filankembo, A.; Giorgio, S.; Lisiecki, I.; Pileni, M. P. Is the Anion the Major Parameter in the Shape Control of Nanocrystals. *J. Phys. Chem. B* **2003**, *107*, 7492–7500.
6. Daniel, M. C.; Astruc, D. Gold Nanoparticles: Assembly, Supramolecular Chemistry, Quantum Size Related Properties and Applications toward Biology, Catalysis, and Nanotechnology. *Chem. Rev.* **2004**, *104*, 293–346.
7. Brust, M.; Walker, M.; Bethell, D.; Schiffrin, D. J.; Whyman, R. Synthesis of Thiol-Derivatized Gold Nanoparticles in a Two-Phase Liquid−Liquid System. *J. Chem. Soc., Chem. Commun.* **1994**, 801–802.
8. Brust, M.; Fink, J.; Bethell, D.; Schiffrin, D. J.; Kiely, C. J. Synthesis and Reactions of Functionalised Gold Nanoparticle. *J. Chem. Soc., Chem. Commun.* **1995**, 1655–1656.
9. Shimizu, T.; Terashini, T.; Hasegawa, S.; Miyake, M. J. Size Evolution of Alkanethiol-Protected Gold Nanoparticles by Heat Treatment in the Solid State. *Phys. Chem. B* **2003**, *107*, 2719–2724.
10. Schadt, M.; Cheung, W.; Luo, J.; Zhong, C. J. Molecularly Tuned Size Selectivity in Thermal Processing of Gold Nanoparticles. *Chem. Mater.* **2006**, *18*, 5147–5150.
11. Maye, M. M.; Zheng, W.; Leibowitz, F. L.; Ly, N. K.; Zhong, C. J. Heating-Induced Evolution of Thiolate-Encapsulated Gold Nanoparticles: A Strategy for Size and Shape Manipulations. *Langmuir* **2000**, *16*, 490–497.
12. Prasad, B. L. V.; Stoeva, S. I.; Sorensen, C. M.; Klabunde, K. J. Digestive Ripening of Thiolated Gold Nanoparticles: The Effect of Alkyl Chain Length. *Langmuir* **2002**, *18*, 7515–7520.
13. Zhou, M.; Chen, S.; Zhao, S. Synthesis of Icosaedral Gold Nanocrystals: A Thermal Process Strategy. *J. Phys. Chem. B* **2006**, *110*, 4510–4513.
14. Alvarez, M. M.; Khoury, J. T.; Schaaff, T. G.; Shafigullin, M.; Vezmar, J.; Whetten, R. L. Critical Sizes in the Growth of Au Clusters. *Chem. Phys. Lett.* **1997**, *266*, 91–98.
15. Ogawa, S.; Ino, S. Formation of Multiply-Twinned Particles in the Nucleation Stage of Film Growth. *J. Vacuum Sci. Technol.* **1969**, *6*, 527–534.
16. Germain, V.; Li, J.; Ingert, D.; Wang, Z. L.; Pileni, M. P. Stacking Faults in Formation of Silver Nanodisks. *J. Phys. Chem. B* **2003**, *107*, 8717–8720.
17. Salzemann, C.; Urban, J.; Lisiecki, I.; Pileni, M. P. Characterization and Growth Process of Copper Nanodisks. *Adv. Funct. Mater.* **2005**, *15*, 1277–1284.
18. Shim, J. H.; Lee, B. J.; Cho, Y. W. Thermal Stability of Unsupported Gold Nanoparticle: A Molecular Dynamics Study. *Surf. Sci.* **2002**, *512*, 262–268.
19. Lisiecki, I.; Sack-Kongehl, H.; Weiss, K.; Urban, J.; Pileni, M. P. Annealing Progress of Anisotropic Copper Nanocrystals: 1—Cylinders. *Langmuir* **2000**, *16*, 8802–8806.
20. Lisiecki, I.; Sack-Kongehl, H.; Weiss, K.; Urban, J.; Pileni, M. P. Annealing Progress of Anisotropic Copper Nanocrystals: 2—Cylinders. *Langmuir* **2000**, *16*, 8807–8808.
21. Yoon, B.; Luedke, W. D.; Gao, J.; Landman, U. Diffusion of Gold Clusters on Defective Graphite Surfaces. *J. Phys. Chem. B* **2003**, *107*, 5882.
22. Bardotti, L.; Jensen, P.; Hoareau, A.; Treilleux, M.; Cabaud, B.; Perez, A.; Cadete Santos Aires, F. Diffusion and Aggregation of Large Antimony and Gold Clusters Deposited on Graphite. *Surf. Sci.* **1996**, *367*, 276.

23. Deltour, P.; Barrat, J. L.; Jensen, P. Fast Diffusion of a Lennard-Jones Cluster on a Crystalline Surface. *Phys. Rev. Lett.* **1997**, *78*, 4597–4600.
24. Landman, U.; Montroll, E. W.; Slesinger, M. F. Motion of Clusters on Surfaces. *Phys. Rev. Lett.* **1977**, *38*, 285–289.
25. Chushak, Y. G.; Bartell, L. S. Melting and Freezing of Gold Nanoclusters. *J. Phys. Chem. B* **2001**, *105*, 11605.
26. Shim, J. H.; Lee, S. C.; Lee, B. J.; Suh, J. H.; Cho, Y. W. Molecular Dynamics Simulation of the Crystallisation of Liquid Gold Nanoparticles. *J. Cryst. Growth* **2003**, *250* 558.
27. Nam, H. S.; Hwang, N. M.; Yu, B. D.; Yoon, J. K. Formation of an Icosahedral Structure During the Freezing of Gold Nanoclusters: Surface-Induced Mechanism. *Phys. Rev. Lett.* **2002**, *89*, 275502-1–275502-4.